

# Design Point Studies for Future Spherical Torus Devices

C. Neumeyer, C. Kessel, M. Peng<sup>a</sup>, P. Rutherford

Princeton Plasma Physics Laboratory,<sup>a</sup> Oak Ridge National Laboratory

*Abstract.* A Systems Code analysis has been developed which provides a tool for the assessment of design points for future spherical torus (ST) devices. The code includes algorithms for plasma physics as well as engineering aspects, which are necessarily simplified but sufficient to capture the essential design-driving considerations. This paper describes the methodology and presents some example cases from ongoing studies.

## I. INTRODUCTION

Systems Codes have been developed at PPPL for study of various tokamak devices [1]. In order to study ST devices, the variant described herein has been developed to capture some of the unique features of the ST configuration. In addition, features are added which account for blanket coverage, tritium breeding, power conversion, and electricity generation. The aim is to provide a tool with which future ST devices such as a Next Step ST (NSST), Component Test Facility (CTF), first demonstration reactor (DEMO), and power reactor can be assessed on a common basis.

## II. PHYSICS LIMITS

Stability limits govern the available range of plasma performance. Reference stability studies by J. Menard et al [2], C. Wong et al [3], and Y. Lin-Liu et al [4] were examined and compared. Results are summarized in Table I.

TABLE I  
PHYSICS LIMITS FROM REFERENCE STABILITY STUDIES

| Variable                           | Menard  | Wong   | Lin-Liu  |
|------------------------------------|---|--|--|
| Max $\kappa$ (A)                   | 1.46155<br>+4.13281 $\epsilon$<br>-2.57812 $\epsilon^2$<br>+1.41016 $\epsilon^3$    | 1.082<br>+2.747/A  |  |
| Min $q_{cyl}$ (A)                  | -0.115479<br>+14.5293 $\epsilon$<br>-27.4492 $\epsilon^2$<br>+18.334 $\epsilon^3$   | 2.0499<br>+0.34791*A   |  |
| $\alpha_n$ (A) =<br>$\alpha_T$ (A) | (0.64-0.3 $\epsilon$ )/2  | 0.25   |  |
| Peakfactor                         | $[\int (1-x)^{2, \alpha_n} dx]^{-1}$<br>$(1-x)^{2, \alpha_n}$<br>$(x=r/a)$          | $[\int (1-x)^{2, \alpha_n} dx]^{-1}$<br>$(1-x)^{2, \alpha_n}$<br>$(x=r/a)$                               |  |
| Max $\beta_N$ (A)                  | (6.96436<br>-14.043 $\epsilon$<br>+45.5 $\epsilon^2$<br>-31.3086 $\epsilon^3$ )/100 | (3.09+3.35/A+<br>3.87/A <sup>0.5</sup><br>*( $\kappa/3$ ) <sup>0.5</sup> /<br>peakfactor) <sup>0.5</sup> | (-0.7748<br>+1.2869 $\kappa$<br>-0.2921 $\kappa^2$<br>+0.0197 $\kappa^3$<br>/(TANH((1.8524<br>+0.2319 $\kappa$ )/A <sup>0.6163</sup> ))<br>A <sup>0.5523</sup> /10 |
| kbs                                | 0.344<br>+0.195*A   | 0.6783<br>+0.0446/A  |  |
| fbs                                | kbs*Beta P*<br>peakfactor <sup>0.25</sup> /A <sup>0.5</sup>                         | kbs*Beta P*<br>peakfactor <sup>0.25</sup> /A <sup>0.5</sup>  |  |

<sup>a</sup> Under US DOE Contract No. DE-AC02-76CHO-3073

In the work described herein we adopt the average of Menard and Wong for the  $\kappa$  limit, Wong for the  $q_{cyl}$  limit, Lin-Liu for the  $\beta_N$  limit, and a constant 0.7 for  $k_{bs}$ .

## III. DESCRIPTION OF ALGORITHMS

Plasma cross sectional shape for 95% flux surface is described by

$$R(\theta) = R_0 + a * \cos(\theta + \delta * \sin(\theta)) \quad (1)$$

$$Z(\theta) = \kappa * a * \sin(\theta)$$

where

$R_0$  = major radius (m)       $\kappa$  = elongation  
 $a$  = minor radius (m)       $\delta$  = triangularity  
 $A$  = aspect ratio =  $R_0/a$        $\theta$  = poloidal angle  
 $\epsilon$  = inverse aspect ratio =  $1/A$

We define  $A_{100}$  and  $a_{100}$  geometric quantities related to the 100% flux surfaces to determine the vacuum vessel geometry based on a linear fit to some sample equilibria by Kessel.

$$\frac{A_{100}}{A_{95}} = (0.017 * A_{95} + 0.932) \quad (2)$$

We assume parabolic profiles raised to a power for density  $\alpha_N$ , temperature  $\alpha_T$ , and NBI power deposition  $\alpha_{NBI}$ .

$$X(r) = X_0 \left[ 1 - \left( \frac{r}{a} \right)^2 \right]^{\alpha_x} \quad (3)$$

For the plasma current calculation,  $\kappa$  is set to maximum allowable,  $q_{cyl}$  is chosen by the solver subject to the minimum allowable and  $B_t$  is varied in the solution process subject to engineering constraints.

$$I_p = \frac{\pi R_0 \epsilon^2 B_t (1 + \kappa^2)}{10^6 q_{cyl} \mu_0} \quad (4)$$

As shown in Fig. 1, the TF coil is assumed to consist of a single turn center-post with flaring at the ends. The dimensions are set according to the following rules.

$$R_{TFmid} = R_0 - a_{100} - \Delta R_{fw} \quad (5)$$

$$R_{TFend} = R_{TFmid} + a_{100}(1 - \delta) \quad (6)$$

$$\Delta Z_{TFmiddle} = 0.9 * \kappa * a_{100} \quad (7)$$

$$\Delta Z_{TFmax} = \kappa * a_{100} + 4.0m \quad (8)$$

Features and constraints on the TF center post design are similar to the ARIES-ST [5] design and as follows.

- Glidcop AL-25 material,  $\sigma=87\%$  IACS
- 60° flaring starting at 90% of the plasma height
- Water inlet temperature of 35°C, flow velocity 10m/s
- Ohmic dissipation and nuclear heating
- Limits on copper and water temperature set at 150°C
- VonMises stresses limited to 100MPa w/concentration factor of 2 to account for cooling passages

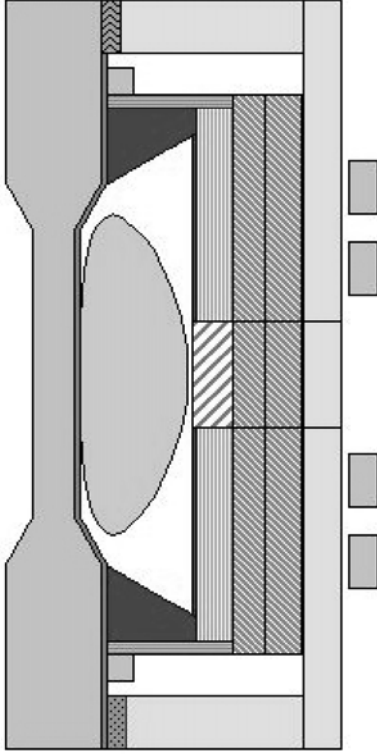


Fig. 1. Cross Section Showing TF Coil and Blanket/Shielding

We assume that the TF current is returned through an aluminum outer shell with horizontal sections typically 1.0m thickness and vertical section 0.75m thick. The following radial builds are assumed between the outer edge of the plasma and the TF return.

- SOL and gap 0.10m
- First wall 0.05m
- Blanket 0.5m
- Shield 0.7m
- Gap 0.1m

These dimensions are noted to be similar to those used for ARIES-ST and should be sufficient to handle 7.5MW/m<sup>2</sup> neutron flux on the outboard midplane.

In the plasma pressure computations,  $\beta_N$  is subject to the physics limit. A calculation toggle is provided for selection between combined ion-electron (global) or separate ion and electron loss channels. In the latter case, separate values are used for the ion and electron pressure. In addition, pressures from fast ions are included. Equations are as follows.

$$\beta_{N\_Total} = \beta_N + \beta_{N\_alpha} + \beta_{N\_nbi} \leq \beta_{N\_Max} \quad (9)$$

$$\beta_N = \beta_{N\_Thermal\_i} + \beta_{N\_Thermal\_e} \quad (10)$$

$$\beta_T = \frac{I_p A \beta_N}{R_0 B_T} = \frac{I_p \beta_N}{R_0 \epsilon B_T} \quad (11)$$

$$\beta_P = \frac{2\beta_T q_{cyl}^2 A^2}{(1 + \kappa^2)} \quad (12)$$

The bootstrap current fraction is based on  $k_{BS}$  and peaking factor per the physics assumptions.

$$f_{BS} = k_{BS} * Peakfactor^{0.25} * \beta_P \sqrt{\epsilon} \quad (13)$$

We assume NBI current drive (positive ion of E<120keV, otherwise negative ion NINB). We set beam energy based on calculations by Mikkelsen showing that the required beam energy for parabolic deposition profiles with tangential injection at  $R_0$  can be approximated as follows.

$$E_b = 100 \langle n_{20} \rangle L_b \quad (14)$$

where

$$L_b = [(R_0 + a)^2 - R_0^2]^{1/2} \quad (15)$$

The current drive efficiency factor is defined as follows.

$$\gamma_{CD} = \frac{n_{20} I_{CD} R_0}{P_{CD}} \quad (16)$$

where

- $\gamma_{CD}$  = efficiency in units 10<sup>20</sup> Ampere/Watt-m<sup>2</sup>
- $n_{20}$  = electron density in units 10<sup>20</sup> Ampere/Watt-m<sup>2</sup>
- $I_{CD}$  = current to be driven in MA
- $P_{CD}$  = current drive power in MW

Data for current drive efficiency from Start and Cordey [6] was curve fit as follows.

$$\gamma_{CDMAX} = E_b^{0.5327} (-8.471 \times 10^{-4} + 1.852 \times 10^{-3} T_{avg} - 5.307 \times 10^{-5} T_{avg}^2) \quad (17)$$

where

- $E_b$  = neutral beam energy
- $T_{avg}$  = average electron temperature

So the current to be driven is  $I_p * (1 - f_{BS})$ , and the power (MW) requirement is

$$P_{CD} = \frac{n_e R_0 I_p (1 - f_{BS})}{10^{20} \gamma_{CD}} \quad (18)$$

Solutions are constrained such that  $\gamma_{CD} \leq \gamma_{CDmax}$  and  $P_{CD} \leq P_{aux}$ .

Power from “thermal” ions and beam-target fusion are integrated over the plasma volume. The alpha power due to “thermal” ions in a 50:50 D-T mix is

$$P_{\alpha 50:50} = 5.6 \times 10^{-25} \int_0^{V_p} [n_{DT}^2(V) e^{a_0 + a_1 T(V) - 0.275 a_1 T(V) + a_2 T(V)^2 + a_3 T(V)^3}] dV \quad (19)$$

where

$$\begin{aligned} a_0 &= -23.836 & a^* &= -22.712 & a_1 &= -0.09393 \\ a_2 &= 7.994e-4 & a_3 &= -3.144e-6 \end{aligned}$$

In general with tritium fraction  $f_T$

$$P_\alpha = P_{\alpha 50:50} * 4 f_T (1 - f_T) \quad (20)$$

For beam-target fusion, curve fits to 400keV were generated to match data from Jassby [7] for  $Q_b$  vs.  $E_b$ . To extend the results out to 1MeV it was assumed based on suggestions from Mikkelsen that  $Q$  should follow a 1/E dependence as

follows and as shown in Fig. 2.

$$Q_{b-E>400keV} = Q_{b-E=400keV} * 400 / E_b \quad (21)$$

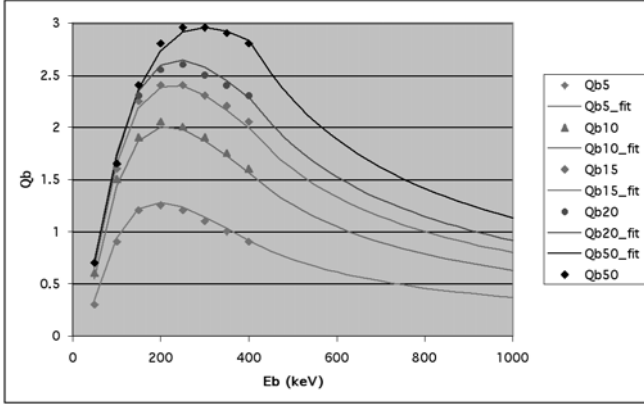


Fig. 2. Fusion Power Gain vs. Eb vs. Background Electron Temperature

Two versions of the energy confinement time are used, namely neoclassical and the ITER 98[y,2] scaling. For the mode where  $T_i=T_e$ , the ITER 98[y,2] scaling is used globally for the ions and electrons. For  $T_i \neq T_e$  the ion confinement is assumed neoclassical and the electrons per the ITER 98 scaling.

Power balance equates net input power to the stored energy divided by the energy confinement time as follows.

$$P_{Tot} = P_\alpha + P_{aux} - P_{rad} = P_\alpha + \frac{P_{fusion}}{Q} - P_{rad} = P_\alpha \left( 1 + \frac{5}{Q} - f_{rad} \right) = \frac{W}{\tau_E} \quad (21)$$

For the mode with separate loss channels and  $T_i \neq T_e$  we have

$$P_{Tot\_e} = P_{\alpha\_e} + P_{aux\_e} - P_{rad} + P_{ie} = \frac{W_e}{\tau_{E\_e}} \quad (22)$$

$$P_{Tot\_i} = P_{\alpha\_i} + P_{aux\_i} - P_{ie} = \frac{W_i}{\tau_{E\_i}} \quad (23)$$

Expressions were derived by Rutherford for partitioning of the alpha and auxiliary power to the ions and electrons, along with an expression for the power flow between ions and electrons.

Concerning heat loads, the power in the scrape off layer is

$$P_{SOL} = P_\alpha + P_{aux} - P_{brem} - P_{line} \quad (24)$$

We assume a double null divertor geometry. Kessel developed models for flux expansion as a function of A which are used to relate  $P_{SOL}$  to the peak divertor heat flux. In our solutions we adjust the radiation fraction at the divertor and enhanced core radiation to suit the allowable peak heat flux on the divertor and first wall. The following constraints are typically applied...

- Allowable peak flux at divertor = 15.0 MW/m<sup>2</sup>
- Allowable peak flux at first wall = 1.0 MW/m<sup>2</sup>

The fraction of neutron flux incident on the center stack was estimated based on line-of-sight considerations as shown in Fig. 3, and the resultant nuclear heating is included in the TF temperature rise calculation. The remaining neutron flux impinges on the first wall.

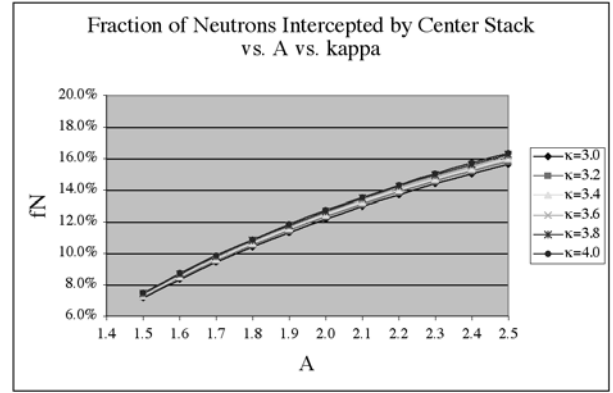


Fig. 3 Neutron flux on Center Stack vs. A vs. kappa

Data was supplied by El Guebaly for n flux distribution on a cylindrical blanket extending up to the plasma height  $\kappa * a$ , based on ARIES-ST work. Weighting functions were then developed which relate the peak to machine average flux on the center stack, divertor, and cylindrical blanket surfaces.

$$A_{pfs} = W_{div} * A_{div} + W_{cs} * A_{cs} + W_{cyl} * A_{cyl} \quad (23)$$

With the weighting functions established, the equation for normalized neutron flux to the outboard region as a function of z (normalized to plasma height) is

$$n_{ob}(z) = W_{cyl} * 1.4318 * (1 - z/1.016) \quad (24)$$

Blanket area is the total plasma facing surface area minus the effective areas of the divertor, center stack, N<sub>nbi</sub> ports for the NBI, and two more for RF, and Diagnostics

$$A_{blanket} = A_{pfs} - (W_{cs} * A_{cs} - W_{div} * A_{div} - W_{port} * dZ_{port} * (2 * 1.0m + N_{nbi} * C_{nbi})) \quad (25)$$

All midplane ports assumed to have the same height of at least 1.0m, and C<sub>nbi</sub> is the width of the chord corresponding to the NBI port. Preferred port height is 1/3 of the plasma but we reserve 1.5m from the top of the plasma (where an outer PF coil will be located) to the top of the port for remote handling

$$dZ_{port} = \text{MIN}(2(\kappa * R_0/A - 1.5), 2\kappa R_0/A/3) \quad (26)$$

For high energy NBI ( $E_b > 120\text{keV}$ ) negative ion injection is required, so current density achievable through the NBI duct is assumed limited to  $J_{nbi}=40\text{A/m}^2$  [8]. For positive ion we assume  $144\text{A/m}^2$  based on the TFTR NBI. These considerations set the number of NBI ports.

Useful thermal power is

$$P_{th} = [P_{neutron} f_{BEM} + (P_\alpha + P_{aux}) f_{rad}] f_{blanket} + k_{div} P_{div} \quad (27)$$

where

$f_{blanket}$  = fraction of surface area covered by blanket

$f_{BEM}$  = blanket energy multiplication factor (assumed =1.2)

$k_{div}$  = toggle used to select divertor power recovery or not

If the toggle is on to generate electricity, gross electrical power production is

$$P_{grosselec} = P_{th} / \eta_{EC} \quad (28)$$

Conversion efficiency  $\eta_{EC}$  is typically assumed 35% for “conventional” power conversion and 45% for “advanced” power conversion cycles. If toggle is on for electricity production, the operation of the “balance of plant” is assumed to consume a fraction ( $f_{BOP}=10\%$ ) of the gross electric power production. Otherwise the balance of plant power is assumed to be 20MW. The net electric power production is

$$P_{netelec} = P_{grosselec} - P_{BOP} - P_{TFinput} - P_{PFinput} - P_{auxinput} \quad (29)$$

The tritium fueling rate per day is

$$Q_{T-fueling} = P_{fusion} / 6.54 \text{ gm/day} \quad (30)$$

Blanket local T breeding ratio TBR is assumed equal to 1.2, so the net fractional breeding ratio (FBR) is

$$FBR = f_{blanket} TBR \quad (31)$$

The net T consumption is...

$$Q_T = (1 - FBR)Q_{T-fueling} \quad (32)$$

#### IV. SOLUTION TECHNIQUE AND RESULTS

We have implanted the algorithms in EXCEL and use the non-linear optimizer SOLVER to find solutions. Typical set of independent variable set adjusted by SOLVER include  $f_{rad}$ ,  $f_{GW}$ ,  $\beta_N$ ,  $q_{cyl}$ ,  $P_{fusion}$ ,  $\eta_{CD}$ ,  $J_{TF}$ ,  $f_w$

Typical set of physics constraints includes the following.

- $f_{rad} \leq P_{brem} / P_{\alpha}$
- $P_{fusion} = 5 * P_{\alpha}$
- $\eta_{CD} \leq \eta_{CDmax} (T) = 0.025 < T >$
- $P_{CD} \leq P_{aux}$
- $\beta_N \leq \beta_{Nmax}$
- $q_{cyl} \geq q_{cylmin}$
- $0.1 \leq f_{BS} \leq \text{specified limit}$
- $0.1 \leq f_{GW} \leq \text{specified limit}$
- $HH = \text{or} \leq \text{an input value}$
- $n_{wall} = \text{or} \leq \text{an input value}$

Additional engineering constraints are applied as appropriate.

High level results from typical calculations are given in Table I for the following cases.

- CTF:           a. 1MW/m<sup>2</sup>,  $E_b=120\text{keV}$   
                   b. 4MW/m<sup>2</sup>,  $E_b>120\text{keV}$   
 DEMO:        100MW net electric  
 REACTOR:    1GW net electric

The results listed represent the minimum major radius

solutions which were found to satisfy all constraints. All cases are at  $A=1.5$ ,  $\kappa=3.2$  and  $\delta=0.6$ .

TABLE I  
SAMPLE CASES

|                           | CTF    | CTF    | DEMO   | REACTOR |
|---------------------------|--------|--------|--------|---------|
| R0[m]                     | 1.20   | 1.20   | 2.50   | 3.00    |
| Bt[T]                     | 2.45   | 2.08   | 1.87   | 1.84    |
| Ip[MA]                    | 9.3    | 12.1   | 21.7   | 24.5    |
| Beta N total              | 4.11%  | 8.26%  | 8.20%  | 7.95%   |
| Beta T total              | 19.6%  | 60.2%  | 57.0%  | 52.9%   |
| Beta P                    | 93.5%  | 132.2% | 156.1% | 149.5%  |
| fGW                       | 18.2%  | 38.3%  | 95.0%  | 91.0%   |
| fBS                       | 60.0%  | 84.8%  | 94.7%  | 90.7%   |
| Tavgj[keV]                | 26.0   | 18.8   | 13.3   | 14.2    |
| Tavge[keV]                | 9.3    | 11.5   | 11.8   | 11.2    |
| HHi                       | 0.13   | 1.00   | 1.00   | 0.50    |
| HHe                       | 0.93   | 1.00   | 0.96   | 0.60    |
| Q                         | 3.2    | 12.6   | 95.8   | 118.6   |
| P fusion[MW]              | 76.6   | 306.5  | 1326.3 | 3194.2  |
| E b[keV]                  | 120.0  | 327.9  | 708.0  | 638.1   |
| Qn tm[MW/m <sup>2</sup> ] | 1.00   | 4.00   | 3.99   | 6.67    |
| FBR                       | 101.9% | 100.8% | 108.9% | 109.3%  |
| P net elec[MW]            | -245.8 | -197.6 | 100.0  | 1000.0  |
| Q elec                    | 0.00   | 0.00   | 1.31   | 3.11    |

#### REFERENCES

- [1] S. Jardin, et al, “Systems Analysis of a Compact Next Step Burning Plasma Experiment”, S Jardin et al, *Fusion Science and Technology*, Vol. 43, March 2003
- [2] J. Menard, et al, "Unified Ideal Stability Limits for Advanced Tokamak and Spherical Torus Plasmas" PPPL Report PPPL-3779
- [3] C. Wong, J. Wesley, R. Stambaugh, E. Cheng, “Toroidal Reactor Designs as a Function of Aspect Ratio and Elongation”, *Nuclear Fusion*, 42 (2002) 547-556
- [4] Y. Lin-Liu and R. Stambaugh, “Optimum Plasma States for Next Step Tokamaks”, GA Report GA-A23980
- [5] W. Reiersen et al, “The TF Coil Design for ARIES-ST”, *Fusion Engineering and Design* 65 (2003) 303-322
- [6] D. Start, J. Cordey, “Beam Induced Currents in Toroidal Plasmas of Arbitrary Aspect Ratio”, *Phys. Fluids*, 23, 1477 (1980)
- [7] D. Jassby, “Neutral Beam Driven Tokamak Fusion Reactors”, *Nuclear Fusion* 17, 309 (1977)
- [8] M. Kuriyama et al, “Operation and Development of the 500keV Negative Ion Based Neutral Beam Injection System for JT60-U”, *Fusion Science and Technology* 42 410 (2002)